Si(001)-2×1 Interfaces

In the photoemission studies of the reaction of the Si (001)-2×1 surface with adsorbates, a great deal of information can be obtained from the analysis of the Si 2p core-level spectra. Success depends critically on first establishing a reliable interpretation of the spectrum obtained from an atomically clean surface. This is not a trivial project, because the reconstruction extends down to the fifth layer for this surface as shown by the low-energy electron diffraction. Ideally then, photoelectron spectroscopy should be able to detect the electronic disturbance of all these layers and exhibit the corresponding surface core-level shifts (SCLSs). In practice, this goal cannot be achieved because the phonon broadening sets a limit to the detection of the small shifts of the deep layers. In fact, published reports using various methods of analysis agree only on the identification of the emission from first two surface layers. The identification of the topmost layer is facilitated by the charge imbalance between the buckled dimer atoms, which splits the surface contribution into two parts with equal intensity and a large energy separation. For these atoms the negative final-state contribution to the SCLS is comparable to the charge-flow shift due to buckling, resulting in a readily resolved up-atom shift. As a result three SCLSs have been amenable to detection in a clean Si 2p core-level spectra.

However, the analysis of high-resolution photoemission spectra clearly shows that additional components are required for a successful representation of the spectral profile. This is in agreement with theoretical final-state calculation of the SCLSs for the Si(001) surface, which shows not only that the screening is enhanced at the surface, but that atoms in the second subsurface layer S(2), i.e., the third layer, encounter different degrees of screening as well. In particular, core holes created in the third layer atoms, lying below the surface dimers (S(2)a), are actually better screened than those created in atoms between the dimer rows (S(2)b). As a result, the third layer contribution is split into two equal parts with a separation reflecting the difference in the final-state core-hole screening.

Six components are consequently required to fit the clean-surface spectra, two each for the surface and the third layer atoms and one each for the second and bulk layer atoms. Experience tells that a unique solution is unlikely to be obtained when so many parameters are required, especially when it is recognized that the phonon width is certainly different in each layer. In order to deal with this problem we have used the layer-wise attenuation due to inelastic scattering to relate the strength of emission from the individual surface layers and the bulk to a single parameter, namely the inelastic mean free path, λ. The results of the data taken at normal and 65° emission with this constraint are shown in Fig. 1, where we have suppressed the $p_{1/2}$ components in order to make the individual contributions easier to be identified. The data were obtained with a 125-mm hemispherical analyzer (OMICRON Vakuumphysik GmbH) in a UHV chamber with the base pressure better than 2.1×10^{-11} Torr. The chamber is stationed at the end of the low-energy spherical grating monochromator (LSGM). The clean Si(001)-2×1 surface was pre-oxidized according to the Ishizaka and Shiraki method, and annealed in a step-wise fashion to 875 ℃ in the photoemission chamber. The silicon sample was held at room temperature during measurements. The SCLSs for the up- and down-dimer atoms (S(0)u and (S(0)d), the first subsurface atom (S(1)), and the two second subsurface layer atoms (S(2)a) and (S(2)b) are −501, −24, +173, −230, and +319 meV, respectively. The corresponding atomic positions can be colorfully referred to Fig. 2(a). An inelastic mean-free-path of 3.32±0.05 Å was also determined by the fitting. Note that the final-state theory for the

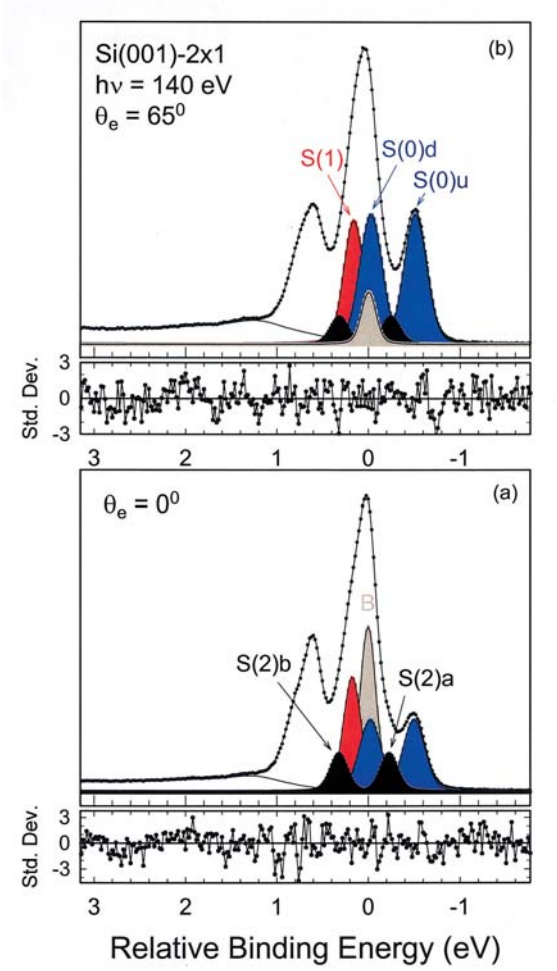

Fig. 1: Simultaneous fit to 150 K data taken for emission angles of 0 and 65˚ .

SCLSs of first three surface layers is in very good agreement with the analysis shown in Fig. 1.

The same method has been applied to determine the kinetic energy dependence of the inelastic mean free path for the Ge(001)-2×1, see Fig. 3.

Once the surface contributions to the Si 2p core level spectra is understood, the interface structures produced by foreign adsorbates can be studied with great confidence and reliability. The results of our studies of Ge, oxygen, and Cl adsorbates, are briefed below. The pressure of the adsorbates was always maintained below 1.0×10^{-10} Torr.

It's long been learned that at low coverage the adsorbed Ge initially replaces the Si dimer up-atoms, while the dimer down-atoms are substituted upon further deposition. In higher thickness, a 2 or 3 ML thick Ge-surface layer is formed. Eventually the nanostructured Ge islands are produced when the coverage exceeds the critical thickness. In addition to this Ge-Ge surface-dimer replacement model, other models as the mixed Ge-Si surface-dimer model and the interface mixing SiGe alloy model were also proposed with considerable acceptance in the literature. The mixed Ge-Si surface-dimer model claimed that only the up atoms in the surface dimers were replaced, while the interface SiGe alloy model postulated that the Ge replacement occurs not only on the top surface layer, but also down below to the next three subsurface layers.

Our photoemission study in submonolayer regime has put these models in question. We have found that the rate of the decrease in component S(0)u is two times faster than that of the increase in the Ge 3d single atom, which conflicts with the one-to-one replacement in the Ge-Ge surface-dimer model. What really happens upon Ge impinging on the silicon surface is that Ge's firstly appear as single, isolated atom at low coverage. They do follow the S(0)u-atoms replacement, which requires considerable amount of energy. Instead, they sit on top of the surface and are captured by S(0)u, as shown as A in Fig. 2(b). Upon further deposition, the neighboring Ge atoms form dimers, as shown as B in Fig.

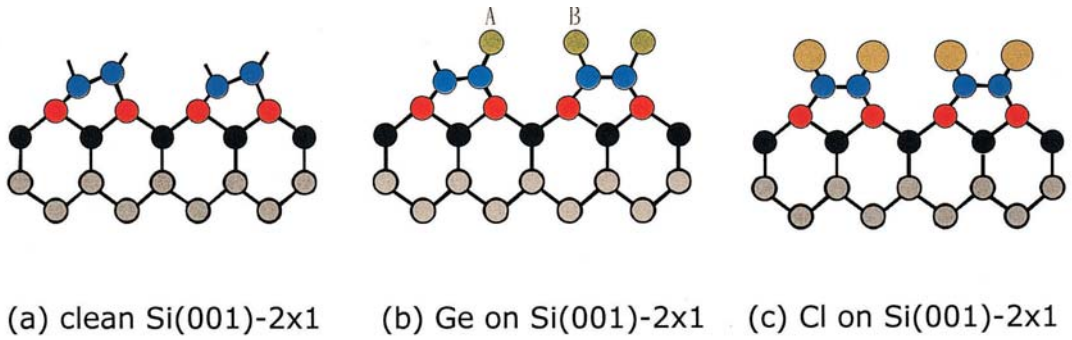

Fig. 2: Schematic side view of the Si(001)-2×1 surfaces, uncovered (a) and covered by Ge (b) and by Cl (c).

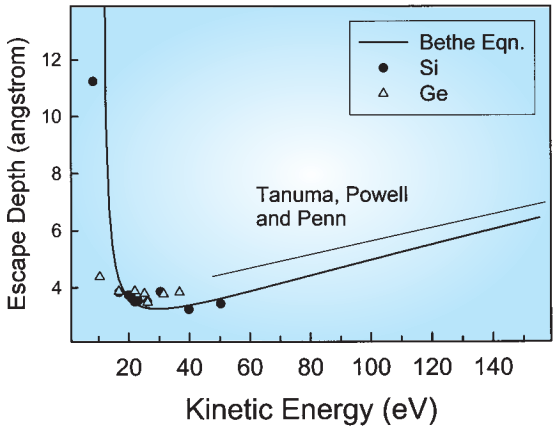

Fig. 3: Inelastic mean-free-path as a function of electron kinetic energy. The data points are the result of our analysis of data of Si and Ge. The Bethe function is $\lambda = E / [E_p^2 \beta \ln(\gamma E)]$, *where* E_p, β, *and* γ *for silicon are16.6 eV, 0.0329, and 0.0919, respectively.*

2(b).

Regarding the chlorine covered Si surface, we have studied both its interface structure and the etching pathway of chlorine on an atomic scale. A fully chlorine-saturated Si surface has been successfully prepared. Its photoemission results, as illustrated in Fig. 4, reveal that at saturation the Si 2p core-level spectra exhibit only a single Cl-induced component with emission twice as strong as that from the Su component of the clean surface and with a positive surface core-level shift of 930±8 meV. The inelastic mean-free-path is 3.4±0.2 Å at a photon energy of 140 eV. The facts that both the surface core-level shift of the first subsurface layer S(1) remains unchanged and the shift of the second subsurface layer S(2) is null as compared with Fig. 2(c), indicate that chlorination removes the strain in the S(2) layer without rupturing the dimer bonds. See Fig. 2(c). Our work finds that the theoretical calculations that involves the Si(001) interfaces must take the contribution from the S(2) layer into account.

Silicon oxide remains the most promising gate oxide material in the next decade. It is projected that by 2012 the gate oxide will be only five silicon atoms thick. In consequence, the growth and morphology of these ultra-thin device-grade oxide films is an issue of great interest. In the literature, both layer-by-layer growth and the existence of a transition range have been proposed to account for the observed behavior. Core-electron photoemission readily resolves the four oxidation states found in the native oxide layer, corresponding to Si atoms with 1, 2, 3 or 4 oxygen neighbors. Oxygen nucleates the growth of small oxide patches, which grow rapidly to a thickness of five atomic layers containing all four oxidation states. In these patches, the farther are the atoms from the silicon surface, the greater are their oxidation states. Upon continuous exposure the patches grow laterally to cover the whole surface.

Although the final-state theory is essential for the proper interpretation of the Si 2p cores in the clean Si(001)-2×1 surface, it is not directly applicable to the analysis of the adsorbate-covered

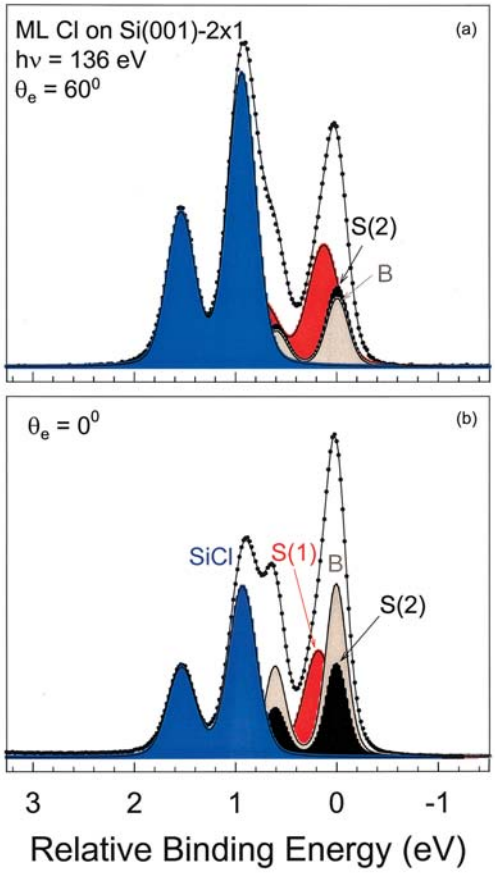

Fig. 4: Result of simultaneous fit to spectra of the Cl-saturated surface taken at 0° and 60° emission angle.

surface. The charges flow between dissimilar atoms in the initial state dominate the SCLSs. Fig. 5 plots the induced SCLSs vs. the differences in electronegativity between the adsorbates and the silicon ($\triangle\chi$), where the shifts are taken from the established high-resolution studies. As can be seen in Fig. 5, the positive correlation between the

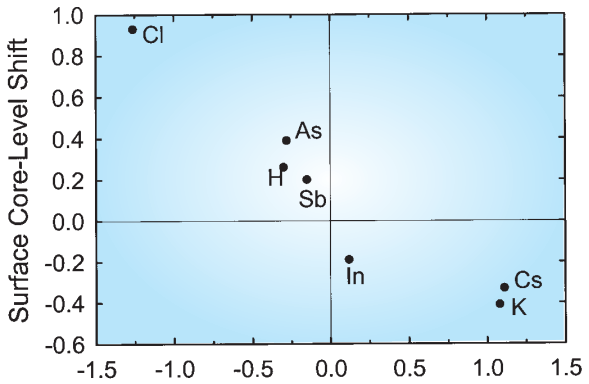

Fig. 5: The induced SCLSs vs. the differences in electronegativity between the adsorbates and the silicon.

induced SCLSs (referred to B) and the differences in electronegativity between the adsorbate and the silicon is well defined, indicating that the initial-state charge transfer upon adsorption overwhelms the screening effect. The measured SCLS alone does not suffice to determine the magnitude of the inevitable final-state contribution. This understanding is relevant to the study of the molecular adsorption, where it may not be clear whether the relevant parameter is the ionization potential or the electron affinity of the molecule as a whole or the formation of a bond with one of the molecular atoms.

One additional benefit of our analytical approach is the ability to clearly differentiate between the emission from the S(1) and S(2) layers. Regardless of the nature of the adsorbate, the S(1) emission remains well separated from the bulk, with a positive SCLS of magnitude not far from that of the clean surface. On the other hand, the SCLS of the S(2) components depends strongly on the electronic properties of the adsorbates and their effect on the buckling. For H, K, Cs, As, Sb, Cl, and Ge, the shifts of the second subsurface layer are 0, −0.17, −0.22, 0, −0.08, 0, and 0 eV, respectively. Although it may seem strange to insist on an unresolved S(2) component with a zero shift in the context of our model function, its addition to the bulk intensity is essential to obtain a meaningful λ. An erroneous λ would interfere with our understanding of the elastic scattering effect of the photoelectrons near the sample surface. It is interesting to note that the average shift of the two S(0) components is negative, while the shift of S(1) remains positive irrespective of the types of the adsorbate.

We have demonstrated that the analysis of Si 2p core-level photoemission spectra provide fruitful information of the interface electronic structures. The capability then enables us to move our foot to the field of the molecular adsorption. Indeed, new results come into sight which will appear in the literature in the coming years.

Beamline:

08A1 Low Energy SGM beamline

Experimental Station:

High-resolution photoemission chamber

Author:

T. W. Pi

National Synchrotron Radiation Research Center, Hsinchu, Taiwan

Publications:

- T.-W. Pi, I.-H. Hong, C.-P. Cheng, G. K. Wertheim, J. El. Spectr. Rel. Phen. **107**, 163 (2000).
- T.-W. Pi, R.-T. Wu, C.-P. Ouyang, J.-F. Wen, G. K. Wertheim, Surf. Sci. **461**, L565 (2000).
- T. -W. Pi, R.-T. Wu, J.-F. Wen, C.-P. Ouyang, and G. K. Wertheim, Surf. Sci. **478**, L333 (2001).
- T.-W. Pi, J.-F. Wen, C.-P. Ouyang, R.-T. Wu, Phys. Rev. B **63**, 153310 (2001).
- T.-W. Pi, S.-F. Tsai, J.-F. Wen, C.-P. Ouyang, Surf. Sci. **488**, 387 (2001).
- T.-W. Pi, C.-P. Ouyang, J.-F. Wen, L.-C. Tien, J. Hwang, C.-P. Cheng, and G. K. Wertheim, Surf. Sci. **514**, 327 (2002).

Contact e-mail:

pi@nsrrc.org.tw